PERGAMON

Available online at www.sciencedirect.com

SCIENCE DIRECT®

Polyhedron 22 (2003) 313–322

POLYHEDRON

www.elsevier.com/locate/poly

Sandwich-type niobium(V) diphthalocyaninato complexes 'stapled' by two inter-ligand C–C σ-bonds. Synthesis and structural investigations of two new phthalocyaninato complexes: $[NbPc_2](IBr_2)$ and $[NbPc_2](IBr_2)\cdot I_2$

Jan Janczak *, Ryszard Kubiak

W. Trzebiatowski Institute of Low Temperature and Structure Research, Polish Academy of Sciences, Okólna 2 str., PO Box 1410, PL-50-950 Wrocław, Poland

Received 19 July 2002; accepted 9 October 2002

Abstract

Two crystals of 1,1′;17,17′-di[phthalocyaninato(2−)] niobium(V) with the composition of $[NbPc_2]IBr_2$ (**1**) and $[NbPc_2]IBr_2\cdot I_2$ (**2**) where $Pc = C_{32}H_{16}N_8$ were grown directly in the reaction of niobium powder with 1,2-dicyanobenzene under a stream of IBr at about 175 °C. An X-ray single-crystal investigations of both crystals indicated sandwich-type structures that are 'stapled' by two inter phthalocyaninato C–C σ-bonds. The anionic part of these complexes was additionally detected by Raman spectroscopy. Magnetic susceptibility and EPR measurements performed on solid state samples indicate a metal-centered monoelectronic oxidation Nb(IV) (with d^1 configuration) → Nb(V) (with d^0 configuration). An absence of the Q band in the UV–Vis spectrum, the typical band for the fully delocalised π-electron aromatic phthalocyaninato(2−) ring system, indicates on the dramatic modification of the chromophore of both complexes, as confirmed by X-ray analysis. Room temperature conductivity measurements performed on several solid samples of **1** and **2** give for both complexes a similar value of $2.5–3.8 \times 10^{-5}\ \Omega^{-1}\ cm^{-1}$. Both crystals are stable in air, but in solution, especially in hot DMSO, both complexes transform into a paramagnetic Nb(IV)Pc_2 complex (d^1 configuration of the central ion).

Keywords: Niobium diphthalocyanine; Niobium(V) complexes; Crystal structures; UV–Vis spectroscopy; 'Stapled' sandwich-type diphthalocyanine; Raman spectroscopy

1. Introduction

A number of metallomono- and diphthalocyanines can be doped with iodine and other oxidizing reagents, forming materials with electrical conducting or semiconducting properties [1,2]. Generally, these properties are strictly connected with the structural and electronic features of the fairly rigid phthalocyaninato macroring, which is the site of extensive π-electron delocalization, as well as on the nature and the electronic structure of the central metal ion. In the iodine-doped metallophthalocyanine materials, the non-integrally (partially oxidized) positively charged metallophthalocyaninato units ($MPc^{\delta+}$ or $MPc_2^{\delta+}$) form pseudo-monodimensional aggregates that are surrounded by the chains of iodine counterions.

An understanding of the charge transport in these partially oxidized materials requires the knowledge of their 'ionicity' i.e. degree of the partial oxidation. Resonance Raman and ^{129}I Mössbauer spectroscopy as well as the diffuse X-ray scattering technique offer simple means for characterizing the anionic polyiodine part of the materials [3]. Extensively theoretical and experimental investigations of these iodine-doped phthalocyaninato complexes suggest two pathways for the charge transport. The high conductivity of these materials is closely related with the structural arrangement which offers strong π–π interaction of neighboring

* Corresponding author. Tel.: +48-71-343-5021; fax: +48-71-441-029

E-mail address: janczak@int.pan.wroc.pl (J. Janczak).

0277-5387/02/$ - see front matter
PII: S0277-5387(02)01305-0

aromatic macrocyclic rings, which are apart below ~3.4 Å, the van der Waals distance of the aromatic carbon atoms [4] as found in organic molecular metals with charge propagation through p–π orbitals of the macrocyclic rings [5]. The second pathway explains the high conductivity by linear-chain metal-spine conductors that propagate charge through the metal character $a_{1g}(d_z^2)$ orbitals [6].

In the course of our studies of metallophthalocyanines we stated that besides this type of iodine doped metallophthalocyaninato complexes in which the iodine doped atoms form chains of symmetrical but disordered triiodide ions, I_3^-, the iodine doped atoms can also form unsymmetrical but ordered triiodide ions as found in $MoOPcI_3$ [7], $SbPcI_3$ [8] and $AsPcI_3$ [9], as well as iodine atoms that can be joined directly to the central metal cation yielding monoiodo- or diiodometallophthalocyaninato complexes [10,11]. Additionally we have stated that iodine doped atoms can form a neutral molecule of I_2, which is a bridge for dimerization or for developing a polymeric structure of mono- and diiodometallophthalocyaninato complexes [12,13].

The new subgroup of sandwich-type metallodiphthalocyaninato complexes in which both phthalocyaninato(2−) macrorings are 'stapled' by two carbon–carbon σ-bonds has not yet been explored enough. There are only two examples of this type of complex that have been structurally characterized [14,15]. Both complexes crystallize with 1-chloronaphthalene molecule as a solvent. To expand the understanding of the solid state properties of the 'stapled' diphthalocyaninato complexes, herein we report the synthesis and structural characterization of new two 'stapled' diphthalocyaninato complexes: $[NbPc_2](IBr_2)$ and $[NbPc_2](IBr_2)\cdot I_2$.

2. Experimental

2.1. Synthesis

All reagents were of the highest grade commercially available and were used as received. The crystals of $[NbPc_2]IBr_2$ (**1**) and $[NbPc_2]IBr_2\cdot I_2$ (**2**) were obtained directly by the reaction of the pure powdered niobium and 1,2-dicyanobenzene under a stream of IBr. The powdered niobium (0.185 g), 1,2-dicyanobenzene (2.050 g) and IBr (0.402 g) in a molar proportion of 1:8:2, with about 5% excess of IBr, were mixed together and pressed into pellets. The pellets were inserted into an evacuated glass ampoule and sealed. The ampoule was heated at about 175 °C for 10 h. At this temperature (175 °C), the liquid 1,2-dicyanobenzene undergoes catalytic tetramerization forming the phthalocyaninato macrocyclic ring, which accepts electrons from niobium, and forms $NbPc_2$ molecules. Simultaneously the IBr additionally oxidized the $NbPc_2$ to $[NbPc_2]^+$ and transforms into IBr_2^- ions and neutral diiodine molecules I_2, that crystallizes with the $[NbPc_2]^+$ yielding two different crystals with the compositions of $[NbPc_2]IBr_2$ and $[NbPc_2]IBr_2\cdot I_2$. The complex of $[NbPc_2]IBr_2$ crystallizes in a parallelepipedal form and the complex of $[NbPc_2]IBr_2\cdot I_2$ in a plate form. The elemental analysis of both complexes has been carried out on an energy dispersive spectrometer. Found for the parallelepiped crystals: C, 54.65; H, 2.26; Br, 14.41; I, 9.10; N, 15.92; Nb, 6.66%. Calc. for $C_{64}H_{32}N_{16}NbIBr_2$: C, 54.72; H, 2.30; Br, 11.38; I, 9.04; N, 15.95; Nb, 6.61%. Found for the plate crystals: C, 46.24; H, 2.00; Br, 9.68; I, 22.32; N, 13.48; Nb, 5.58%; and Calc. for $C_{64}H_{32}N_{16}NbIBr_2\cdot I_2$: C, 46.35; H, 1.95; Br, 9.64; I, 22.95; N, 13.51; Nb, 5.60%.

2.2. X-ray crystallography

The X-ray single-crystals of $[NbPc_2]IBr_2$ and $[NbPc_2]IBr_2\cdot I_2$ with dimensions of $0.22\times0.14\times0.12$ and $0.34\times0.14\times0.06$ mm, respectively, were used for data collection on a four-circle KUMA KM-4 diffractometer equipped with a two-dimensional area CCD detector. The graphite-monochromatized Mo Kα radiation ($\lambda = 0.71073$ Å) and ω-scan technique with $\Delta\omega = 0.75°$ for one image were used for data collection. The 960 images for six different runs covering about 95% of the Ewald sphere were performed. The lattice parameters were determined by the least-squares methods on the basis of all reflections with $F^2 > 2\sigma(F^2)$. One image was monitored as a standard after every 40 images. Integration of the intensities, correction for Lorentz and polarization effects, were performed using KUMA KM-4 CCD software [16]. The face-indexed analytical absorption was calculated using SHELXTL program [17]. A total of 22 828 (6449 independent, $R_{int} = 0.0419$) and 44 667 (14 062 independent, $R_{int} = 0.0149$) reflections were performed for the crystals of $[NbPc_2]IBr_2$ and $[NbPc_2]IBr_2\cdot I_2$, respectively. The structures were solved by the Patterson heavy-atom method and refined by the full-matrix least-squares method using the SHELXL-97 program [18] with anisotropic thermal parameters for all non-hydrogen atoms (for H atoms the $U_{iso} = 1.2U_{iso}$, i.e. 20% higher than the carbon atom directly bonded the H atom). The final difference Fourier maps showed no peaks of chemical significance. The largest peaks are $+1.235/-0.629$ and $+0.763/-0.498$ e $Å^{-3}$ for the complexes of $[NbPc_2]IBr_2$ and $[NbPc_2]IBr_2\cdot I_2$, respectively. The details of the data collection and final refinement parameters are listed in Table 1. Selected bond lengths and angles are summarized in Table 2.

2.3. Physical measurements

Measurements of the electronic spectra of both complexes were carried out at room temperature (r.t.)

Table 1
Crystallographic data for $[NbPc_2]IBr_2$ and $[NbPc_2]IBr_2 \cdot I_2$

Compound	$[NbPc_2]IBr_2$ (**1**)	$[NbPc_2]IBr_2 \cdot I_2$ (**2**)
Chemical formula	$[Nb(C_{32}H_{16}N_8)_2]IBr_2$	$[Nb(C_{32}H_{16}N_8)_2]IBr_2 \cdot I_2$
Formula weight	1404.69	1658.49
Space group	$C2/c$ (No. 15)	$P2_1/c$ (No. 14)
Radiation (λ, Å)	Mo Kα (0.71073)	Mo Kα (0.71073)
a (Å)	18.863(4)	11.330(2)
b (Å)	19.327(4)	23.868(5)
c (Å)	16.553(3)	22.027(4)
β (°)	115.37(3)	100.73(3)
V (Å^3)	5352.7(19)	5852.5(19)
T, (°C)	293(2)	293(2)
d_{calc} (g cm^{-3})	1.711	1.882
d_{obsd} (g cm^{-3})	1.71	1.88
μ, (mm^{-1})	2.313	3.212
Z	4	4
R_1 [$F^2 > 2\sigma(F^2)$] [a]	0.0372	0.0644
wR_2 (F^2 all reflections) [b]	0.0573	0.0618
Goodness-of-fit, S	1.008	0.994

[a] $R = \Sigma||F_o|-||F_c||/\Sigma\ F_o$.
[b] $wR = \{\Sigma[w(F_o^2-F_c^2)^2]/\Sigma wF_o^4\}^{1/2}$; $w^{-1} = \sigma^2(F_o^2)+(0.0160P)^2$ for $[NbPc_2]IBr_2$ and $w^{-1} = \sigma^2(F_o^2)+(0.0086P)^2$ for $[NbPc_2]IBr_2 \cdot I_2$ where $P = (F_o^2+2F_c^2)/3$.

using a Cary-Varian 2300 spectrometer. The UV–Vis spectra were recorded from CH_2Cl_2 solution in 0.5 cm quartz cell. The Raman spectra were recorded at r.t. in a Jobin–Yvon Ramanor U-1000 spectrometer equipped with a photomultiplier-type detector and phonon-counting hardware. The 90° geometry was used. An argon-laser line at 514.5 nm, of power 100 mW, was used as the exciting radiation. Resolution was set up to 3 cm^{-1}. The magnetic susceptibility measurements were carried out on a Quantum Design SQUID magnetometer (San Diego, CA). The EPR measurements were recorded on ESP 300 E-Bruker X-band spectrometer. R.t. conductivity measurements were carried out on several polycrystalline compacted samples pressed into pellets by using a standard four-point probe technique [19].

3. Result and discussion

3.1. Synthesis and characterization

In contrast to the preparation method of the 'stapled' metallodiphthalocyaninato complexes described in the literature which leads to the crystal with chloronaphthalene as solvent molecules 14a15b, our preparation method leads directly to good-quality single crystals suitable for X-ray structure analysis without any solvent molecules. The oxidation of phthalocyaninato ring Pc(2−) → Pc(1−) ($E_o = 714(4)$ mV) by I_2 is well known [20], and has been widely used for obtaining the partially oxidized metallophthlalocyaninato and diphthalocyaninato complexes [1,2]. IBr is a stronger oxidant than I_2

Table 2
Selected bond lengths (Å) and angles (°)

Bond lengths			
[NbPc$_2$]IBr$_2$			
I1–Br1	2.7465(11)	I1–Br1a	2.7465(11)
Nb–N1	2.194(2)	Nb–N3	2.337(2)
Nb–N5	2.190(2)	Nb–N7	2.241(2)
C1–C1a	1.640(5)	C17–C17a	1.619(5)
Pc ring			
N1–C1	1.489(3)	N1–C8	1.334(3)
N2–C8	1.330(3)	N2–C9	1.315(3)
N3–C9	1.379(3)	N3–C16	1.437(3)
N4–C16	1.272(3)	N4–C17	1.436(3)
N5–C17	1.500(3)	N5–C24	1.359(3)
N6–C24	1.326(3)	N6–C25	1.310(3)
N7–C25	1.369(3)	N7–C32	1.440(3)
N8–C1	1.436(3)	N8–C32	1.271(3)
Bond angles			
Br1–I1–Br1a′	176.03(2)	N1–Nb–N3	74.29(8)
N1–Nb–N5	121.39(7)	N1–Nb–N7	74.02(7)
N3–Nb–N5	74.07(7)	N3–Nb–N7	111.75(7)
N5–Nb–N7	73.87(7)	N1–C1–C1a	100.2(2)
N8–C1–C1a	107.4(2)	C2–C1–C1a	114.0(2)
Symmetry code: (a) $-x$, y, $3/2-z$; (a′) $-1-x$, y, $3/2-z$.			
Bond lengths			
[NbPc$_2$]IBr$_2$·I$_2$			
I1–I3	2.703(2)	I2–Br1	2.686(2)
I2–Br2	2.818(2)	I1–Br1	3.066(1)
Nb–N1a	2.166(3)	Nb–N1b	2.222(3)
Nb–N3a	2.263(3)	Nb–N3b	2.263(3)
Nb–N5a	2.173(3)	Nb–N5b	2.192(3)
Nb–N7a	2.213(4)	Nb–N7b	2.265(3)
C1a–C1b	1.638(6)	C17a–C17b	1.588(6)
Pc ring (A)			
N1a–C1a	1.448(6)	N1a–C8a	1.372(5)
N2a–C1a	1.405(5)	N2a–C32a	1.307(5)
N3a–C32a	1.406(5)	N3a–C25a	1.384(5)
N4a–C25a	1.309(5)	N4a–C24a	1.339(5)
N5a–C24a	1.351(4)	N5a–C17a	1.484(5)
N6a–C17a	1.441(5)	N6a–C16a	1.268(5)
N7a–C16a	1.471(5)	N7a–C9a	1.364(5)
N8a–C9a	1.319(5)	N8a–C8a	1.421(5)
Pc ring (B)			
N1b–C1b	1.483(5)	N1b–C8b	1.333(5)
N2b–C8b	1.332(5)	N2b–C9b	1.347(5)
N3b–C9b	1.270(5)	N3b–C16b	1.466(5)
N4b–C16b	1.243(5)	N4b–C17b	1.390(5)
N5b–C17b	1.516(5)	N5b–C24b	1.340(5)
N6b–C24b	1.311(5)	N6b–C25b	1.325(5)
N7b–C25b	1.346(5)	N7b–C32b	1.461(5)
N8b–C32b	1.254(5)	N8b–C1b	1.385(5)
Bond angles			
Br1–I2–Br2	176.7(2)	Br1–I1–I3	176.3(2)
I1–Br1–I2	93.8(2)	N1a–Nb–N3a	73.0(1)
N1a–Nb–N5a	123.6(1)	N1a–Nb–N7a	76.2(1)
N3a–Nb–N5a	74.5(1)	N3a–Nb–N7a	112.6(1)
N5a–Nb–N7a	75.5(1)	N1b–Nb–N3b	73.0(1)
N1b–Nb–N5b	120.9(1)	N1b–Nb–N7b	74.5(1)
N3b–Nb–N5b	73.7(1)	N3b–Nb–N7b	111.1(1)
N5b–Nb–N7b	74.1(1)	N1a–Nb–N1b	71.4(1)
N1a–Nb–N3b	139.7(1)	N1a–Nb–N5b	142.6(1)
N1a–Nb–N7b	76.5(1)		
N3a–Nb–N1b	76.3(1)	N3a–Nb–N3b	80.9(1)

N3a–Nb–N5b	141.7(1)	N3a–Nb–N7b	143.0(1)
N5a–Nb–N1b	140.0(1)	N5a–Nb–N3b	75.9(1)
N5a–Nb–N5b	72.0(1)	N5a–Nb–N7b	141.5(1)
N7a–Nb–N1b	142.0(1)	N7a–Nb–N3b	143.3(1)
N7a–Nb–N5b	76.0(1)	N7a–Nb–N7b	79.2(1)

[21]. The synthesis of $[NbPc_2]IBr_2$ and $[NbPc_2]IBr_2 \cdot I_2$ from the phthalonitrile and powdered pure niobium under a stream of IBr requires the formation of the heterotrihalide IBr_2^- ions and neutral I_2 molecules. Usually the IBr_2^- ion is synthesized by the reaction of I^- with Br_2 [22]. However, under our reaction conditions the IBr_2^- ion is the result of the heterolitic thermal dissociation of IBr [21]. The formation of the complexes can be written as:

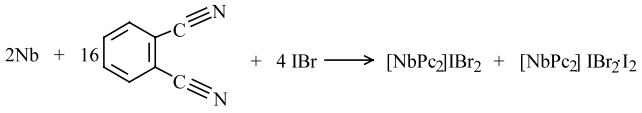

Both obtained complexes are not soluble in any of the usual solvents (water, acetone and alcohol), but are slightly soluble in pyridine, DMF, DMSO and in high boiling aromatic solvents like chloronaphthalene or quinoline. However, after several days black–brown powder materials were obtained from the solution in DMSO. The magnetic susceptibility measurement performed on this powder material indicates paramagnetism ($\mu_{eff} = 1.71\mu_B$). The elemental analysis of this powder material is consistent with the $NbPc_2$ complex (Nb(IV), d^1 configuration), that has been characterized earlier by spectroscopic methods 15a. Thus it was found that the decomposition process of both complexes and formation of the paramagnetic $[NbPc_2]$ complex takes place in solution. This process depends strongly on the temperature, and takes place several times quicker in hot solvents.

3.2. Description of the structures

The molecular structures of **1** and **2** with the labeling scheme of the atoms is illustrated on Figs. 1 and 2, respectively. Both sandwich-type $[NbPc_2]$ units consist of two saucer-shaped phthalocyaninato ligands, that surround the niobium cation, which is located closely in the center of $[NbPc_2]$ in **1**, since the molecule has a twofold symmetry axis, while in **2** the niobium cation is slightly displaced from the center of the $[NbPc_2]$ unit (1.133 and 1.184 Å from the N_4 plane of the A and B Pc rings, respectively). In both complexes due to the staggered orientation of the two phthalocyaninato macrorings (relative rotation 45°), the inner N_4 isoindole system is arranged around the central niobium cation in the form of a square antiprism. Among the sandwich-type metallodiphthalocyaninato complexes, these two niobium complexes are the unique ones in which the

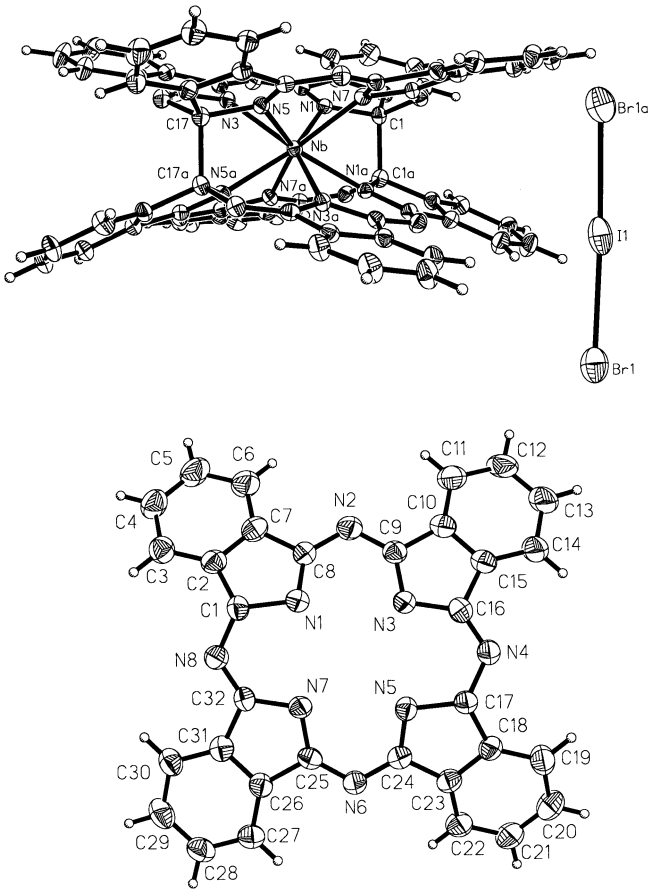

Fig. 1. Molecular structure of $[NbPc_2]IBr_2$, a side view (a) and the labelling of the atoms in the phthalocyanininato ring (b). Displacement ellipsoids are shown at the 50% probability level.

most characteristic and peculiar feature is the presence of two C–C σ-bonds [C1–C1a, C17–C17a in **1** and C1a–C1b, C17a–C17b in **2**, see Figs. 1 and 2], that staple together both phthalocyaninato macrorings at opposite sides of the niobium cation. This results, first, in the sp^3 hybridization of the C-head atoms bridging the two macrocycles, with a consequent breaking of the extensive π-electron delocalization system present in the normal phthalocyaninato skeleton, and second, in the closest observed distance of the two inner N_4–N_4 isoindole planes (see Table 3). The inter-ligand σ C–C bond lengths are significantly longer [C1–C1a = 1.640(5) Å, C17–C17a = 1.619(5) Å in **1** and C1a–C1b = 1.638(6) Å, C17a–C17b = 1.588(6) Å in **2**] than the expected value of 1.530(15) Å for a normal C–C σ-bond [23]. The elongation of these 'stapled' C–C σ-bonds is undoubtedly due to the π–π interaction between the macrocyclic rings. Each one of the four C sp^3 head atoms forms four single σ-bonds, thus partially breaking the π-delocalization system, otherwise it is fully extended on the macrocyclic Pc ring. Figs. 1(b) and 2(b) show the phthalocyaninato macrocyclic rings with the designations of the atoms. As a result of the interruption

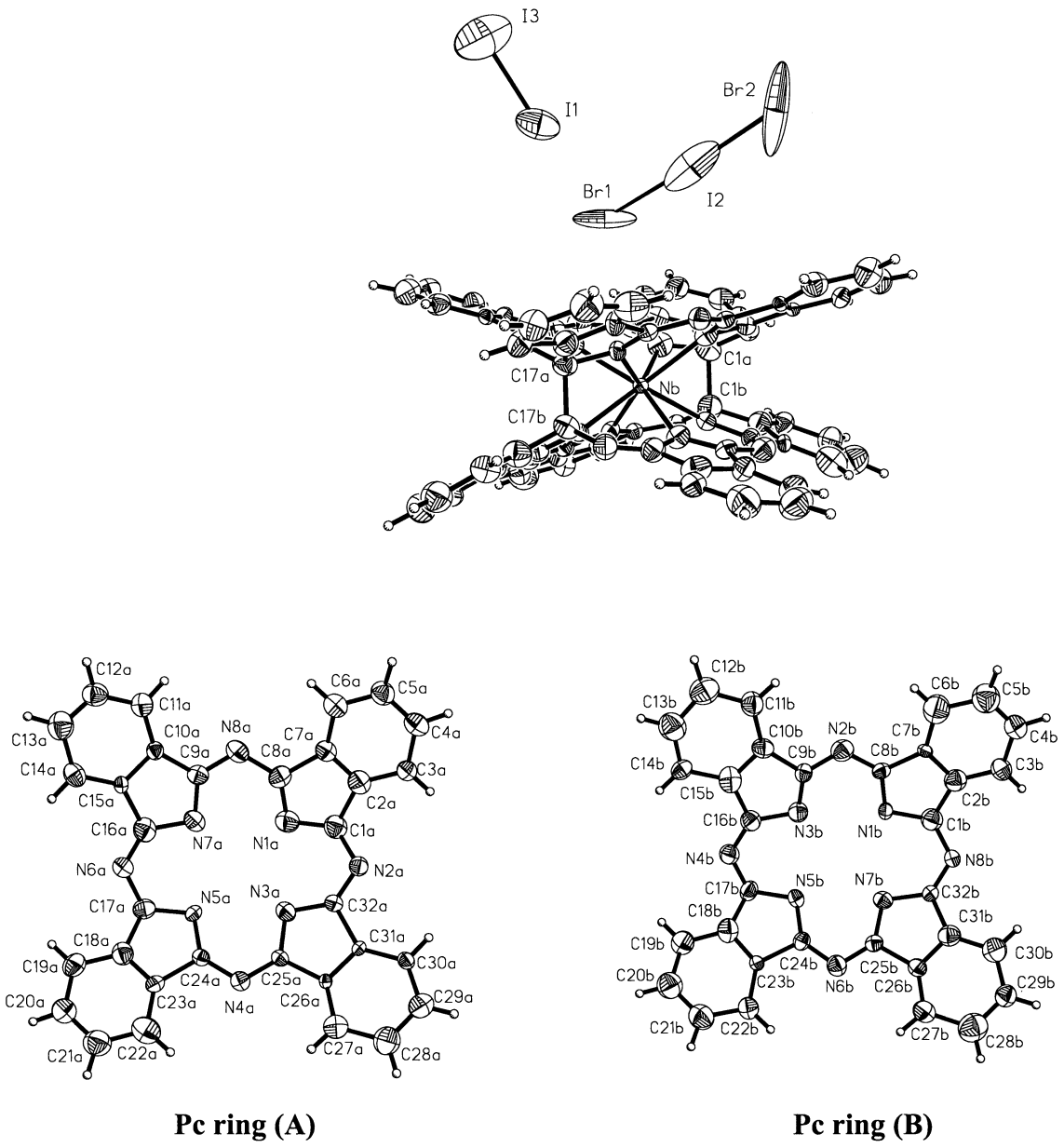

Fig. 2. Molecular structure of $[NbPc_2]IBr_2 \cdot I_2$, a side view (a) and the labelling of the atoms in the phthalocyaninato rings (b). Displacement ellipsoids are shown at the 50% probability level.

Table 3
Comparison of the coordination of the central metal cation in the 'stapled' metallodiphthalocyaninato complexes

Complex	Average $M-N_{isso}$ (Å)	Distance between N_4-planes	Rotation of the ring (°)	Formal oxidation state	Ionic radius [a] for CN = 8 (Å)	References
$[TiPc_2]ClNP$ [b]	2.21	2.32	45	4+	0.74	[14a]
$[NbPc_2]I_3(I_2)ClNP$	2.22	2.39	45	5+	0.74	[15b]
$[NbPc_2]IBr_2$	2.21	2.331(5)	45	5+	0.74	This work
$[NbPc_2]IBr_2 \cdot I_2$	2.20	2.148(6)	45	5+	0.74	This work
$[ZrPc_2]$	2.30	2.52 [c]	42	4+	0.84	[24]

[a] From reference [25].
[b] ClNP = 1-chloronaphtlalene.
[c] This distance was given as 2.20 Å in Ref. [24] (see discussion).

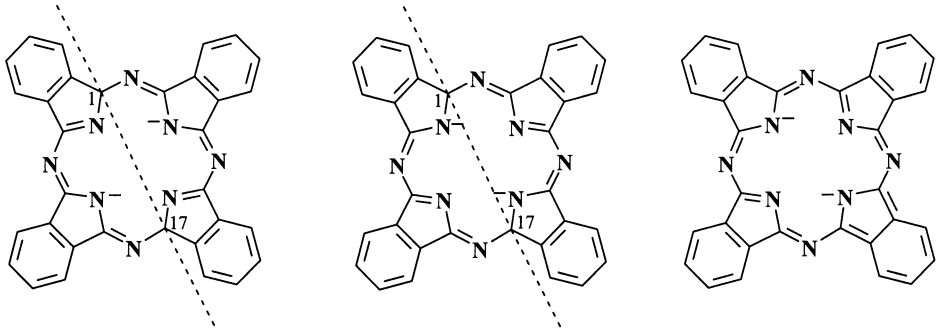

Scheme 1.

of the π-electron delocalization, the two possible alternative forms for each individual phthalocyaninato ring in the [$NbPc_2$] unit are illustrated in Scheme 1. The chemical diagrams (I) and (II) represent the different distribution of the localization of the 'double' and 'single' bonds within the macrocyclic ring. The X-ray single crystal structure analysis of **1** definitely indicates diagram (I) as the representation approached by the complex of [$NbPc_2$]IBr_2, since the inner ring clearly locates the 'double' and 'single' on the both sides of the dotted line passing through the C1 and C17 atoms, although the aromaticity of the peripheral benzo rings is less perturbed. The crystal structure of **2** accommodates both diagrams (I) and (II) as representations of the phthalocyaninato macrorings [ring A—(I) and ring B—(II)], since both Pc macrorings in this case are crystallographically independent. According to representation (I), two pairs of opposite Nb–$N_{isoindole}$ bonds are formed, in the crystal of **1**, one with shorter Nb–$N_{isoindole}$ [Nb–N1, Nb–N1a = 2.194(2) Å and Nb–N5, Nb–N5a = 2.190(2) Å] and another with longer Nb–$N_{isoindole}$ distances [Nb–N3, Nb–N3a = 2.237(2) Å and Nb–N7, Nb–N7a = 2.241(2) Å]. The longer Nb–$N_{isoindole}$ bonds are apparently associated with more ionic bonds, while the shorter with a more covalent character of the bonds. In the crystal of **2** the relation between the longer and shorter Nb–$N_{isoindole}$ bonds is slightly disturbed by the interaction of the [$NbPc_2$] unit with the anionic part of the complex ($IBr_2^-\cdot I_2$), since it interacts differently on each side of the [$NbPc_2$] unit; on one side Br1 is interacting with the Pc ring, on the other side of the [$NbPc_2$] unit the Pc ring is interacting with the I3 and Br2 atoms of the I_2 and IBr_2^- units, respectively. Furthermore, the representations (I) and (II) have 18 double bonds, which differ from the 19 ones present in the normal phthalocyaninato skeleton (diagram III). Therefore, the formation of the two inter-ring C–C σ-bonds corresponds to the breaking of one out of the nineteen double C=C bonds in each 'normal' phthalocyaninato unit and is an isomerization process, which can be schematically represented as a cycloaddition:

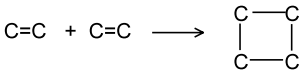

and not a redox one as discussed in details in the paper describing the 'stapled' diphthalocyaninato titanium complex [14a].

Due to the interruption of the π-electron delocalization and sp^3 character of the two carbon atoms, the planarity of the phthalocyaninato macrocycles is completely removed. This distortion is responsible for the back-to-back facing of the saucer-shaped macrocyclic rings and can be estimated by the bending of the isoindole units with respect to the N_4-core and by the 'twisting' of the peripheral phenyl rings (Table 4). As can be seen from Table 4 the phthalocyaninato rings in the crystal of **2** are more perturbed than in **1**. The interplanar N_4–N_4 distance of 2.331(5) Å in the crystal of **1** is comparable with those found in the crystal of [$NbPc_2$]$I_3(I_2)_{0.5}\cdot 3.5ClNP$ [15b] and in the crystal of [$ZrPc_2$] (~2.32 Å) [14a], while in the crystal of **2** the interplanar N_4–N_4 distance is significantly shorter (2.148(6) Å) than those in the above mentioned complexes, and can be explained by the repulsive interaction of both the phthalocyaninato rings of the [$NbPc_2$] unit with the anionic parts of the complex ($IBr_2^-\cdot I_2$) that are located in the crystal on both sides of the [$NbPc_2$] unit. Among the sandwich-type metallodiphthalocyanines without the inter-ring C–C σ-bonds, the closest N_4–N_4 distance can be found in $ZrPc_2$ [24]. However, the reported interplanar N_4–N_4 distance of ~2.20 Å in $ZrPc_2$ is not clear, since using the normal procedure to calculate this distance from the positional parameters given in [24] yields 2.52 Å. The shortest interplanar N_4–N_4 distance in $ZrPc_2$ within the 'normal' metallodiphthalocyaninato complexes can be explained by the relatively small ionic radius (Zr^{4+} = 0.74 Å, CN = 8) [25].

The arrangement of molecules of [$NbPc_2$]IBr_2 and [$NbPc_2$]$IBr_2\cdot I_2$ in the crystals **1** and **2** is illustrated in Figs. 3 and 4, respectively. The structure of [$NbPc_2$]IBr_2 consists of columnar stacks along a *c*-axis of positively charged [$NbPc_2$]$^+$ units, well separated from the almost

Table 4
Distortion of the phthalocyaninato rings in $[NbPc_2]IBr_2$ and $[NbPc_2]IBr_2 \cdot I_2$

Compound	Bending of the isoindole [a] with respect to the N_4 plane (°), e.s.d's = 0.02				'Twisting' of the external phenyl ring given by the displacement of the outer most carbon atoms of the phenyl ring (Å), e.s.d.'s. = 0.01							
	N1	N3	N5	N7	C4	C5	C12	C13	C20	C21	C28	C29
$N[NbPc_2]IBr_2$	25.7	18.1	25.4	9.9	1.01	1.41	1.53	1.34	1.05	1.44	0.91	0.91
$[NbPc_2]Ibr_2 \cdot I_2$ [b]	24.9	13.0	20.9	11.9	1.03	1.44	1.85	1.82	0.73	1.10	1.43	1.21
	25.3	18.3	26.4	18.2	0.80	1.30	1.54	1.37	1.11	1.50	1.52	1.32

[a] The isoindole containing N1, C1–C8, N3, C9–C16, N5, C17–C24 and N7, C25–C32.
[b] The first line relating to the (A) Pc ring, the second the (B) Pc ring.

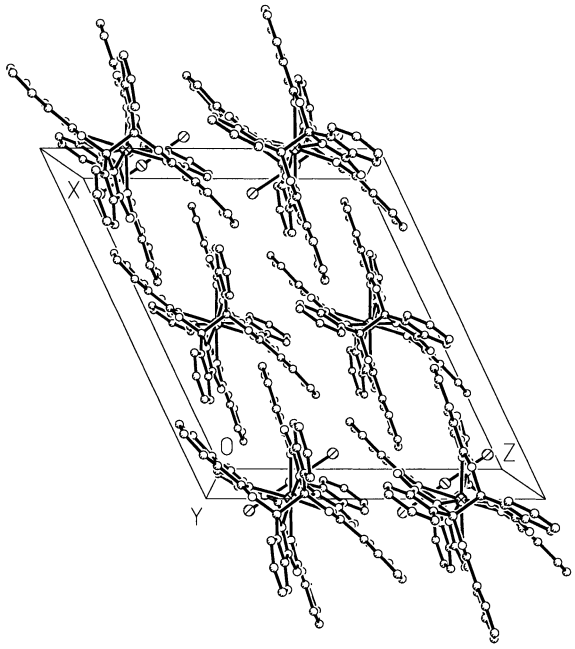

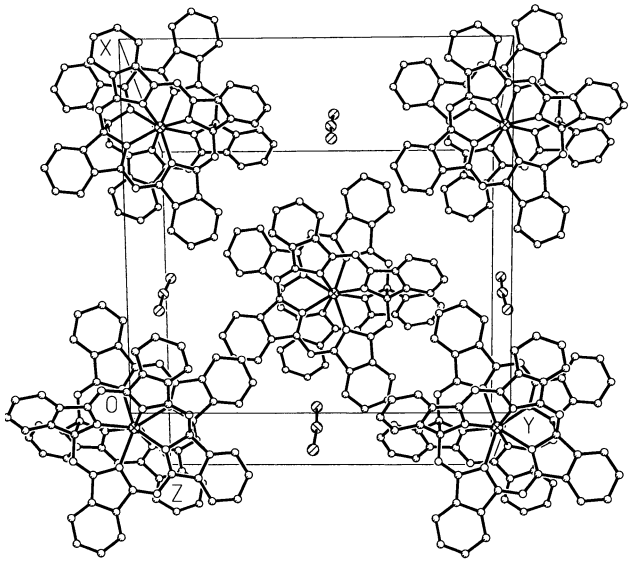

Fig. 3. Arrangement of $[NbPc_2]IBr_2$ molecules in the crystal lattice.

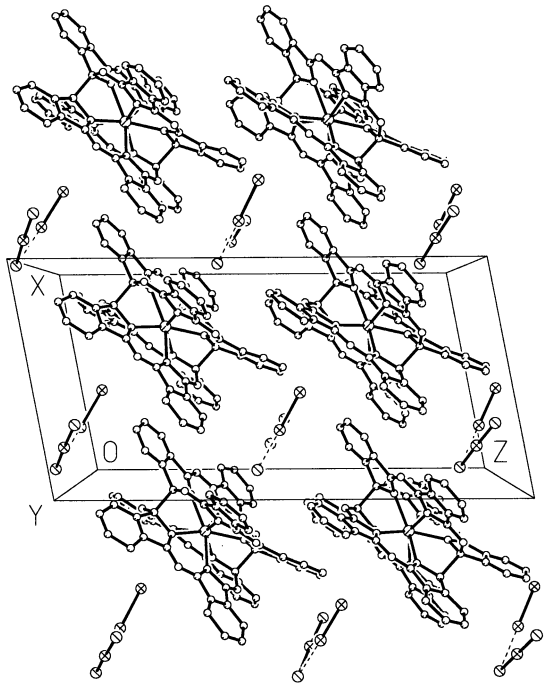

Fig. 4. Crystal structure of $[NbPc_2]IBr_2 \cdot I_2$ showing the alternating arrangement of oppositely charged $[NbPc_2]^+$ and $IBr_2^- \cdots I_2$ moieties.

linear heterotrihalide ions of IBr_2^-, that are located in the channels between the $[NbPc_2]^+$ units. In the crystal of **2** the arrangement of the oppositely charged $[NbPc_2]^+$ and $(IBr_2 \cdot I_2)$ units is different than in **1**. The interacting $IBr_2^- \cdots I_2$ aggregates are located on both sides of the $[NbPc_2]^+$ units and interact with the Pc rings (Fig. 4). This is undoubtedly the reason for the much more perturbed Pc rings as well as for the slightly asymmetric location of the Nb cation in the $[NbPc_2]$ unit. The heterotrihalide IBr_2^- ions in both crystals are almost linear, the I–Br–I angle is equal to 176.03(2)° and 176.29(3)° in the crystals of **1** and **2**, respectively. In the crystal of **1** the IBr_2^- ion is symmetric, while in the crystal of **2** it is asymmetric due to the interaction with the neutral I_2 molecule (Scheme 2). This interaction leads to the elongation of one I–Br bond with simultaneouse shortening of the other I–Br bond in relation to the 'non-interacting' symmetrical IBr_2^- as found in the

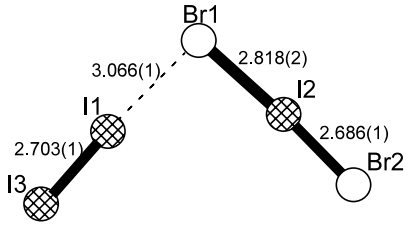

Scheme 2.

crystal **1**. The mutual arrangement of I_2 and IBr_2^- (Scheme 2) suggests the existence of the $I_3Br_2^-$ anionic fragment, however, the I–I value of 2.703(1) Å for the neutral molecule of I_2 (2.712(15) Å in pure crystalline iodine, [26]) indicates the existence of the neutral I_2 molecule in the crystal, which is only slightly interacting with the heterotrihalide IBr_2^- ion. This is in agreement with the Raman experiment described below.

3.3. Physical properties

Room temperature conductivity measurements performed on several solid samples of **1** and **2** give for both complexes a similar value of $2.5–3.8 \times 10^{-5}\ \Omega^{-1}\ cm^{-1}$, indicating semiconducting properties. The conductivity of these two complexes ($[NbPc_2]IBr_2$ and $[NbPc_2]IBr_2 \cdot I_2$) is greater by a factor of 10^3 compared with the conductivity of the $[NbPc_2]$ complex measured on polycrystalline compacted samples ($2.2–3.0 \times 10^{-8}\ \Omega^{-1}\ cm^{-1}$) at room temperature. The visible spectra in dichloromethane solution of $[NbPc_2]IBr_2$ and $[NbPc_2]IBr_2 \cdot I_2$ show intense absorption in the B region. Fig. 5 shows the spectra of both 'stapled' Nb-diphthalocyanines with $NbPcCl_2$ as a representation of a 'normal' phthalocyanine. The spectra of 'stapled' Nb-complexes are practically identical and exhibit two

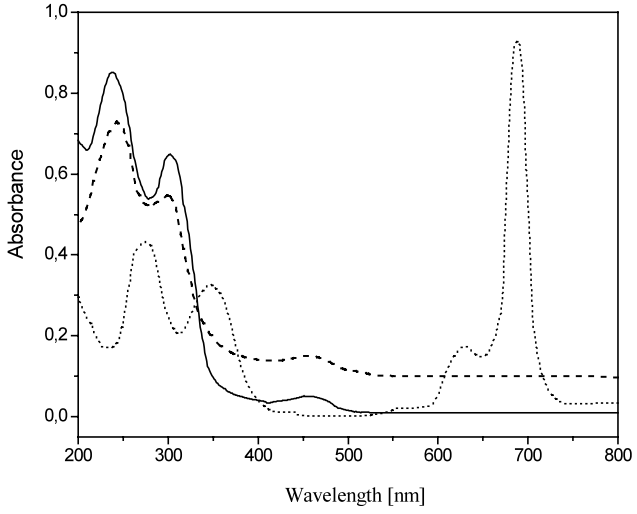

Fig. 5. UV–Vis spectra in CH_2Cl_2 solution of $[NbPc_2]IBr_2$ (solid line), $[NbPc_2]IBr_2 \cdot I_2$ (dashed line) and 'normal' phthalocyanine $NbPcCl_2$ for a comparison.

Table 5
UV–Vis solution spectra in CH_2Cl_2 of the 'stapled' niobiumdiphthalocyaninato complexes

Complex	λ (nm), $\varepsilon \times 10^4$ ($dm^3\ mol^{-1}\ cm^{-1}$)	Reference
$[Nb(V)Pc_2]IBr_2$	247 (10.23); 305 (8.92); ~455 (0.77)	this work
$[Nb(V)Pc_2]IBr_2 \cdot I_2$	251 (9.67); 308 (7.43); ~455 (0.75)	this work
$[Nb(V)Pc_2]I_3(I_2)ClNP$ [a]	253 (8.82); 303 (7.45)	[16b]
$[Nb(IV)Pc_2]$	251 (11.2); 298 (12.3)	this work

[a] Very weak shoulders at about 335 and 480 nm were also observed.

intense absorptions in the near-UV region (200–350 nm), one weak band at about 455 nm and the complete absence of a Q band in the region of 550–800 nm, usually observed and responsible for the blue–green color of the phthalocyanine system in general (see Fig. 5, the spectrum of $NbPcCl_2$). The visible spectral data (Table 5) indicate on the interruption of the aromaticity (breaking the delocalization of the π-electron system), and a dramatic modification of the chromophore as confirmed by the X-ray analysis. This is also the reason of the brown color of these crystals.

The oxidation process of the initially formed $[NbPc_2]$ molecule by the IBr, in contrast to the oxidation by I_2 which normally leads to the partially oxidation of the phthalocyaninato rings and the formation of the tetragonal crystals of metallomonphthalocyaninato or diphthalocyaninato complexes [1,2], is metal-centered monoelectronic oxidation $Nb^{4+} \rightarrow Nb^{5+} + e$, since the EPR and magnetic susceptibility measurements indicate diamagnetic character (Nb^{5+}, d^0 configuration). If the oxidation process takes place on the macrocyclic phthalocyaninato ring, the complexes **1** and **2** should be EPR active and in solution the hyperfine structure due to the coupling of the unpaired electron with the nuclear spin as for the $Nb(IV)Pc_2$ complex (Nb^{4+}, d^1 configuration, nuclear spin of Nb, I = 9/2) should be observed.

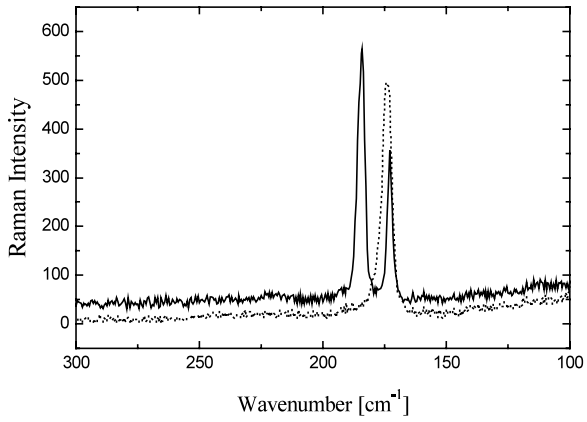

Fig. 6. Raman spectra of the solid-state sample of $[NbPc_2]IBr_2$ (dotted line) and $[NbPc_2]IBr_2 \cdot I_2$ (solid line).

The Raman spectrum of $[NbPc_2]IBr_2$ (Fig. 6) exhibits only one band at $\sim 172\ cm^{-1}$ that indicate IBr_2^- ions, which well correlate with the expected value of 168 cm^{-1} for IBr_2^- [27], while in the spectrum of $[NbPc_2]IBr_2 \cdot I_2$, besides the band attributed to the IBr_2^- ions ($\sim 170\ cm^{-1}$), one additional band at $\sim 185\ cm^{-1}$ is observed, that corresponds to the weakly interacting neutral I_2 molecule as observed in the other complexes containing the neutral I_2 molecule [12,13,28].

4. Concluding remarks

1) The oxidation of the initially formed paramagnetic $[NbPc_2]$ complex by IBr is a metal-centered monoelectronic process yielding two diamagnetic complexes with the composition of $[NbPc_2]IBr_2$ and $[NbPc_2]IBr_2 \cdot I_2$.
2) Interruption of the fully delocalization of the aromatic π-electron system by two C–C σ-bonds is responsible for the change of the UV–Vis spectrum.
3) The 'stapled' by two inter-ring C–C σ-bonds sandwich-type complexes are formed only by metals with a high oxidation state (Ti^{4+}, Nd^{4+}, and Nd^{5+}) and relatively small ionic radius.
4) Due to the sp^3 character of the 'stapled' carbon atoms an alternating location of 'double' and 'single' bonds on the both side of the C-head atoms is observed.
5) The unoxidised complex of $[NbPc_2]$, as shown by the UV–Vis spectrum, is also in a 'stapled' sandwiched form.

5. Supplementary material

Crystallographic data for the structures reported in this paper have been deposited with the Cambridge Crystallographic Data Center as supplementary publication No. CCDC-185484 and CCDC-185485. Copies of the data can be obtained free of charge on application to The Director, CCDC, 12 Union Road, Cambridge CB2 1EZ, UK (fax: +44-1223-336033; e-mail: deposit@ccdc.cam.ac.uk or www: http://www.ccdc.cam.ac.uk).

Acknowledgements

This work was supported by a grant (No. 3 T09A 180 19) from the Polish State Committee for Scientific Research.

References

[1] (a) C.J. Schramm, R.P. Scaringe, D.R. Stojakovic, B.M. Hoffman, J.A. Ibers, T.J. Marks, J. Am. Chem. Soc. 102 (1980) 6702;
(b) J.A. Ibers, L.J. Pace, J. Martinsen, B.M. Hoffman, Struct. Bonding (Berlin) 50 (1982) 1;
(c) B.M. Hoffman, J.A. Ibers, Acc. Chem. Res. 16 (1983) 15;
(d) B.N. Diel, T. Inabe, J.W. Lyding, K.F. Schoch, Jr., C.R. Kannewurf, T.J. Marks, J. Am. Chem. Soc. 105 (1983) 1551;
(e) K. Yakushi, M. Sakuda, H. Kuroda, A. Kawamoto, J. Tanaka, Chem. Lett. (1986) 1161.;
(f) T. Inabe, J.G. Gandiello, M.K. Moguel, J.W. Lyding, R.L. Burton, W.J. McVarthy, C.R. Kannewurf, T.J. Marks, J. Am. Chem. Soc. 108 (1986) 7595;
(g) M. Safarpour-Haghihi, H. Rath, H.W. Rotter, H. Homborg, Z. Anorg. Allg. Chem. 619 (1993) 1897;
(h) G. Ostendorph, H.W. Rotter, H. Homborg, Z. Anorg. Allg. Chem. 622 (1996) 235.
[2] (a) J. Janczak, R. Kubiak, F. Hahn, Inorg. Chim. Acta 281 (1998) 195;
(b) J. Janczak, R. Kubiak, Polyhedron 18 (1999) 1621;
(c) J. Janczak, R. Kubiak, A. Jezierski, Inorg. Chem. 38 (1999) 2043;
(d) J. Janczak, R. Kubiak, I. Svoboda, A. Jezierski, H. Fuess, Inorg. Chim. Acta 304 (2000) 150;
(e) J. Janczak, Y.M. Idemori, Inorg. Chim. Acta 325 (2001) 85.
[3] (a) T.J. Marks, Ann. New York Acad. Sci. (1978) 594.;
(b) M. Cowie, A. Gleizes, G.W. Grynkiewich, D.W. Kalina, M.S. McClure, R.P. Scarinnge, R.C. Teitelbaum, S.L. Ruby, J.A. Ibers, C.R. Kannewurf, T.J. Marks, J. Am. Chem. Soc. 110 (1979) 2921.
[4] L. Pauling, The Nature of the Chemical Bond, Cornell University Press, Ithaca, NY, 1960, p. 262.
[5] (a) C.J. Schramm, D.J. Stojakovic, B.M. Hoffman, T.J. Marks, Science 200 (1978) 47;
(b) T.J. Marks, Science 227 (1985) 881.
[6] (a) J.M. Williams, A.J. Schultz, A.E. Underhill, K. Carneiro, Extended Linear Chain Compounds, vol. 1, Plenenum Press, New York, 1982, pp. 73–118;
(b) M.C. Bohm, One Dimensional Organometallic Materials, Lecture Notes in Chemistry, vol. 48, Springer, Berlin, 1987.
[7] J. Janczak, R. Kubiak, Inorg. Chem. 38 (1999) 2429.
[8] R. Kubiak, J. Janczak, M. Razik, Inorg. Chim. Acta 293 (1999) 155.
[9] J. Janczak, Y.M. Idemori, Acta Crystallogr., Sect. E 58 (2002) m36.
[10] (a) J. Janczak, R. Kubiak, Inorg. Chim. Acta 288 (1999) 174;
(b) K. Ejsmont, R. Kubiak, Acta Crystallogr., Sect. C 54 (1988) 1844;
(c) K. Schweiger, H. Hückstadt, H. Homborg, Z. Anorg. Allg. Chem. 624 (1998) 167;
(d) J. Janczak, Y.M. Idemori, Acta Crystallogr., Sect. C 57 (2001) 924.
[11] (a) K. Ejsmont, R. Kubiak, Acta Crystallogr., Sect. C 53 (1997) 1051;
(b) J. Janczak, R. Kubiak, Polish J.Chem. 73 (1999) 1587.
[12] J. Janczak, R. Kubiak, F. Hahn, Inorg. Chim. Acta 287 (1999) 101.
[13] J. Janczak, M. Razik, R. Kubiak, Acta Crystallogr., Sect. C 55 (1999) 359.
[14] (a) C. Ercolani, A.M. Paoletti, G. Penesi, G. Rossi, A. Chiesi-Villa, C. Rizzoli, J. Chem. Soc., Dalton Trans. (1990) 1971.;
(b) A. Capobianchi, C. Ercolani, A.M. Paoletti, G. Penesi, G. Rossi, A. Chiesi-Villa, Inorg. Chem. 32 (1993) 4605.
[15] (a) M.P. Donzello, C. Ercolani, P.J. Lukes, Inorg. Chim. Acta 256 (1997) 171;

(b) M.P. Donzello, C. Ercolani, A. Chiesi-Villa, C. Rizzoli, Inorg. Chem. 37 (1998) 1347.
[16] KUMA KM-4 CCD Software, Ver. 163, User's Guide, Wroclaw, Poland, 1999.
[17] G.M. Sheldrick, SHELXTL Program, Siemens Analytical X-ray Instrument Inc, Madison, WI, 1990.
[18] G.M. Sheldrick, SHELXL-97, Program for the Solution and Refinement of Crystal Structures, University of Göttingen, Göttingen, Germany, 1997.
[19] T.E. Phillips, J.R. Anderson, C.J. Schramm, B.M. Hoffman, Rer. Sci. Instrum. 50 (1979) 263.
[20] T. Inabe, T.J. Marks, R.L. Burton, J.W. Lyding, W.J. McCarthy, C.R. Kannewurf, G.M. Reisner, F.H. Herbstein, Solid State Commun. 54 (1985) 501.
[21] N.N. Greenwood, A. Earnshaw, Chemistry of the Elements, Pergamon Press, New York, 1989.
[22] A.I. Popoc, R.E. Buckles, in: T. Moeller (Ed.), Inorganic Syntheses, vol. 5, McGraw-Hill, New York, 1957, pp. 167–175.
[23] F.H. Allen, O. Kennard, D.G. Watson, L. Brammer, A.G. Orpen, R. Taylor, J. Chem. Soc., Perkin Trans. 2 (1987) S1.
[24] J. Silver, P. Lukes, S.D. Howe, B. Howlin, J. Mater. Chem. 1 (1991) 29.
[25] R.D. Shannon, Acta Crystallogr., Sect. A 32 (1976) 751.
[26] F. van Bolhuis, P.B. Kostner, T. Migchelsen, Acta Crystallogr. 23 (1967) 90.
[27] J.R. Ferraro, M.A. Beno, R.J. Thorn, H.H. Wang, K.S. Webb, J.M. Williams, J. Phys. Chem. Solids 47 (1986) 301.
[28] (a) R.C. Teteibaum, S.I. Ruby, T.J. Marks, J. Am. Chem. Soc. 100 (1978) 3215;
(b) R.C. Teteibaum, S.I. Ruby, T.J. Marks, J. Am. Chem. Soc. 102 (1980) 3222.